Numerical analysis and centrifugal modeling of LNAPLs transport in subsurface system*

HU Liming[1]**, LO I. M. C.[2] and MEEGODA J. N.[3]

(1. Department of Hydraulic Engineering, Tsinghua University, Beijing 100084, China; 2. Department of Civil Engineering, Hong Kong University of Science and Technology, Hong Kong SAR, China; 3. Department of Civil and Environmental Engineering, New Jersey Institute of Technology, USA).

Received July 11, 2005; revised November 6, 2005

Abstract The transport of non-aqueous phase liquids (NAPLs) in unsaturated soils and groundwater is an important research topic in geo-environmental engineering. In this paper, the mechanism of light NAPLs (LNAPLs) transport in subsurface system is briefly introduced, and the mass transport equations, fluid flow equations, and the constitutive model of relative permeability - saturation - capillary pressure are discussed. Then the numerical method is introduced to simulate the multiphase flow problems in porous media, and the tempo-spatial distribution of LNAPLs is obtained. Moreover, different boundary conditions are employed in numerical simulation to investigate its effect on transport behavior. To verify the numerical data, centrifugal tests are conducted to model the LNAPLs migration in unsaturated soils and groundwater. The calculation results are agreeable with the experimental findings of centrifugal modeling, which indicates that LNAPLs from leaking point move downwards due to gravity force, and form a high concentration zone above the capillary fringe, and then spread out laterally along the groundwater table. Some LNAPL enters groundwater system to further migrate. The combination of numerical simulation and centrifuge modeling can be a useful means to study the transport behavior of LNAPLs in subsurface system.

Keywords: geo-environmental engineering, subsurface contamination, multiphase flow, light non-aqueous phase liquids (LNAPLs), centrifugal modeling technique, numerical simulation.

The installation of millions of underground storage tanks (USTs) for storing hazardous materials has posed a serious threat to soil and groundwater quality as well as to public health and welfare. Many hazardous chemicals in petroleum hydrocarbons are nearly immiscible in water and named non-aqueous phase liquids (NAPLs). Light NAPLs (LNAPLs) have specific gravities less than water and often migrate into the unsaturated zone of a soil-water-air system. To establish the most effective soil remediation technology that can be utilized in the control of releases from leaking USTs and to minimize unreasonable risks to human health and the environment, it is essential to investigate the transport behavior and contamination extent of LNAPLs in subsurface system.

To date, investigation of the flow and transport of LNAPLs in subsurface systems has used approaches such as laboratory studies, numerical modeling, and field investigation. Conventional laboratory studies, though relatively uncomplicated to perform, are often inadequate for simulating site conditions and the long-term transport of LNAPLs in the vadose zone and in groundwater. Field investigations are rarely completed in a single stage and usually require several phases after revisions based on previous investigation. The amount of time needed to run field tests is extensive and the total resources required for site investigations are expensive.

Numerical modeling seems to be a cost-effective means since it can simulate various initial/boundary conditions as well as the long-term migration behavior. Several numerical models have been developed to simulate subsurface contamination problems[1,2]. However, the LNAPL transport in subsurface system is a very complicated process. Besides the complex multiphase flow in porous media, the transport behavior of LNAPL is affected by various effects such as dissolution, volatilization, adsorption, degradation, as well as convection and dispersion effect in groundwater and air phase. It is difficult to develop such an appropriate mathematical model to account for all of these processes because of the difficulty in obtaining accurate input parameters for the model.

In recent years, the geotechnical centrifuge has

* Supported by National Natural Science Foundation of China (Grant No. 50209006), European Community Asia-Link Programme (Contract No. CN/ASIA-LINK/010 94-556), and the Tsinghua Basic Research Fund

** To whom correspondence should be addressed. E-mail: gehu@tsinghua.edu.cn

been used effectively to study contaminant transport in soils[3—11]. Scaling laws governing the relationship between a centrifuge model and its corresponding prototype have been developed to establish model dimensions[12,13], as listed in Table 1. Due to the scaling laws for centrifuge, a field event that lasts decades may be simulated within hours in the centrifuge. The centrifuge data are often used to verify the numerical solutions. However, the agreement between calculation results and experimental data is not satisfactory due to the difficulties of multiphase flow and inaccurate model parameters[4,8].

Table 1. Scaling factors for pollutant transport problems

Symbol	Description	Dimension	Scale
L	Length	L	1/N
m	Mass	M	$1/N^3$
ρ	Density	ML^{-3}	1
γ	Unit weight	$ML^{-2}T^{-2}$	N
g	Gravity	LT^{-2}	N
P	Pressure	MLT^{-2}	1
v	Flow velocity	LT^{-1}	N
t	Time	T	$1/N^2$
k	Permeability	LT^{-1}	N
V	Volume	L^3	$1/N^3$

The objective of this study is to model the transport process of LNAPLs in subsurface system and to investigate the migration patterns. The numerical simulation and the centrifuge experiment were designed to simulate LNAPL transport from a leaky underground storage tank and its subsequent migration into the subsurface system. Tempo-spatial distribution of LNAPLs is obtained, and the comparison between numerical and experimental data is carried out to investigate the transport behavior. Furthermore, the effect of boundary conditions is also discussed.

1 Theoretical approach of LNAPL transport in subsurface system

LNAPLs transport in subsurface system is a very complicated process, as shown in Fig. 1. When LNAPL is spilled at the ground surface, it enters the unsaturated zone under the earth's gravity. Upon encountering a capillary fringe, the LNAPL forms a pancake-like layer above the saturated zone. Groundwater flowing past the floating LNAPL dissolves soluble components, forming a dissolved plume down-gradient of the LNAPL zone. Since air, water and NAPL are immiscible with each other, there exists a three-phase flow in porous soil mass.

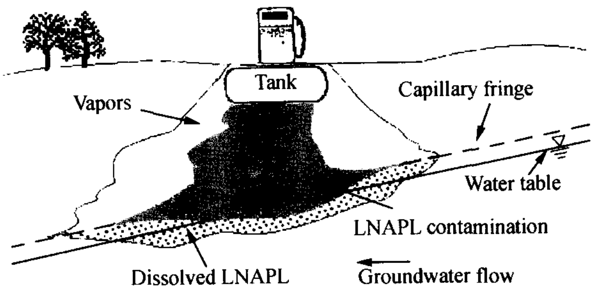

Fig. 1. LNAPLs release and Subsequent Migration.

The mathematical model for multi-phase flow in porous medium consists of three main components: the mass balance equations which define the distribution in time and space of each fluid species, the fluid flow equations which describe the flow velocity of each fluid in the system, and the constitutive equations of k-S-P which define the inter-relationship of capillary pressure, saturation and relative permeability.

1.1 Mass balance equations

In the air-water-NAPL-soil system, there are five types of fluid constituents, i.e. (w, W), a water species in the water phase (free water phase); (n, W), an NAPL species in water phase (dissolved NAPL in water phase); (n, N), an NAPL species in NAPL phase (free NAPL phase); (n, G), an NAPL species in the gas phase (dissolved NAPL in gas phase); and (g, G), a gas species in the gas phase (free gas phase). The mass balance law for each fluid constituent can be expressed as the following equation[14]:

$$\frac{\partial(\varepsilon S_\alpha \rho_\iota^\alpha)}{\partial t} + \nabla \cdot [\varepsilon S_\alpha \rho_\iota^\alpha \boldsymbol{v}^\alpha] - \nabla \cdot \left[\varepsilon S_\alpha \rho^\alpha \boldsymbol{D}^\alpha \cdot \nabla\left(\frac{\rho_\iota^\alpha}{\rho^\alpha}\right)\right] = \rho_\iota^\alpha Q^\alpha + \hat{\rho}_\iota^\alpha, \quad (1)$$

where the order pair (ι, α) represents a species ι in a fluid phase α, i.e. (w, W), (n, W), (n, N), (n, G), and (g, G). ε is the porosity of the porous medium; S_α the saturation of the α phase; ρ_ι^α the mass concentration of species ι in the α-phase $[M/L^3]$; $\boldsymbol{v}_\alpha$ the mass average velocity vector of phase $\alpha [L/T]$; $\boldsymbol{D}_\alpha$ the second-order tensor of dispersion coefficient for the α-phase $[L^2/T]$. $\rho_\iota^\alpha Q^\alpha$ represents the point source or sink, and $\hat{\rho}_\iota^\alpha$ is the mass source or sink due to inter-phase mass exchange $[M/L^3T]$.

There are four forms of LNAPL in subsurface system: free phase of LNAPL; NAPL in gas phase due to volatilization; NAPL in water phase due to dissolution; NAPL adsorbed in solid phase. The main processes of mass exchange pertinent to NAPL are dissolution, volatilization and sorption.

1.2 Fluid flow equations

There are three independent flowing fluids in this system, i.e. water, air and NAPL. Assuming that unsaturated flow of each fluid phase follows Darcy's law and Richards' equation[15], the velocity of each fluid phase can be written in terms of multiphase extension:

$$\boldsymbol{v}^{\alpha} = -\frac{\boldsymbol{k}k_r^{\alpha}}{\varepsilon S_{\alpha}\mu^{\alpha}} \cdot (\nabla P^{\alpha} - \gamma^{\alpha} \nabla z), \tag{2}$$

where P^{α} is the α-phase pressure $[\mathrm{MLT}^{-2}]$, μ the dynamic viscosity of fluid phase $[\mathrm{MLT}^{-1}]$, and γ^{α} the specific weight of the α-phase $[\mathrm{ML}^{-2}\mathrm{T}^{-2}]$. The intrinsic permeability tensor $\boldsymbol{k}\,[\mathrm{L}^2]$ is a function of medium fabric, and independent of fluid properties. k_r is the relative permeability, i.e. the ratio of the effective permeability of a fluid at a given saturation to the intrinsic permeability of the medium, $0 \leqslant k_r \leqslant 1$, which is a scaling factor.

The permeability of each fluid is one of the most important parameters to be obtained, which is related to fluid saturation and capillary pressure. The constitutive relationship of relative permeability, saturation and capillary pressure is one of the most important mechanisms governing the transport behavior in porous media.

1.3 Constitutive relationship of relative permeability - saturation - capillary pressure

With respect to modeling the three-phase flow in porous media, there exists a substantial amount of researches defining appropriate constitutive relationships. In water-NAPL-air system, it is often assumed that the fluid wettability from the most to least is water, NAPL and gas. Water is the most wetting phase, and it spreads as a film over the soil grains. NAPL has intermediate wettability, and it spreads as a film over the water. Gas is the least wetting phase and it is surrounded by the total wetting phases, i.e. water and NAPL. The three-phase k-S-P model can be idealized as two inter-related sub-models: saturation - capillary pressure, and relative permeability - saturation.

1.3.1 Saturation-capillary pressure (S-P) sub-model

The S-P model describes the functional relationship between saturation and capillary pressure. Three-phase S-P model can be decomposed into two two-phase models. In water-NAPL system, NAPL is considered as a non-wetting phase, and in NAPL-gas system, NAPL is a wetting phase. Several S-P models were developed in the past years in terms of unsaturated soil of water-air system[16—19], which are indicated by the soil-water characteristic curve, as shown in Fig. 2. Moisture retention expressions in the unsaturated flow are extended to account for the presence of the NAPL phase[20—22]. By assuming that the pair capillary pressure in the three-fluid system is related to the interfacial tension and each fluid, the two phase S-P model can be extended to describe the three-phase system.

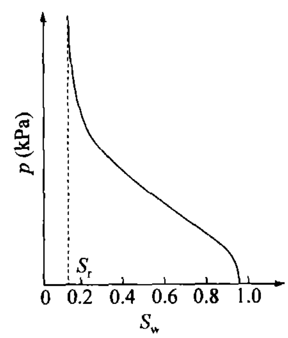

Fig. 2. Soil water characteristic curve.

With respect to the NAPL phase, since the trapping mechanisms are different for wetting and non-wetting phases, the magnitude of trapped NAPL can be considered as a function of displacing phases. In water-NAPL-air system, the residual saturation of NAPL (S_{Nr}) can be defined as a linear function of water and gas saturations[23]:

$$S_{Nr} = S_{Nwr}\left(\frac{S_G}{S_W + S_G}\right) + S_{Nnr}\left(\frac{S_G}{S_W + S_G}\right), \tag{3}$$

where S_{Nnr} indicates the NAPL residual saturation as a non-wetting phase, and S_{Nwr} represents the NAPL residual saturation as a wetting phase.

1.3.2 Relative permeability-saturation (k-S) sub-model

The k-S model describes the functional relationship between relative permeability and saturation. Several k-S models were developed to describe the permeability for air-water-soil system of unsaturated soils[17,24—27]. Considering the two-phase system with water and NAPL, the variation of the relative permeability with effective saturation should be that shown in Fig. 3. For the three-phase system, relative permeability of each fluid is usually presented in a ternary diagram (Fig. 4)[28].

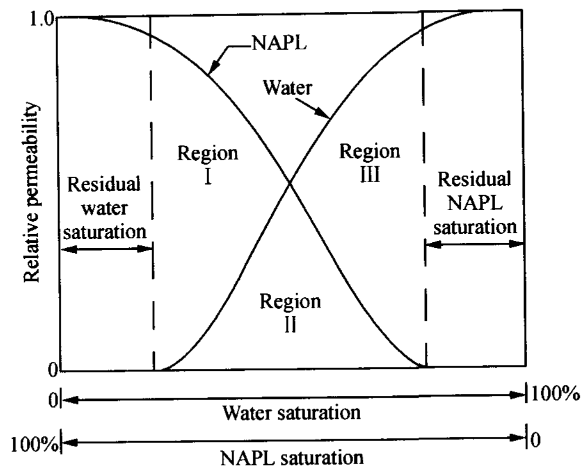

Fig. 3. Relative permeability of water and NAPL as a function of saturation.

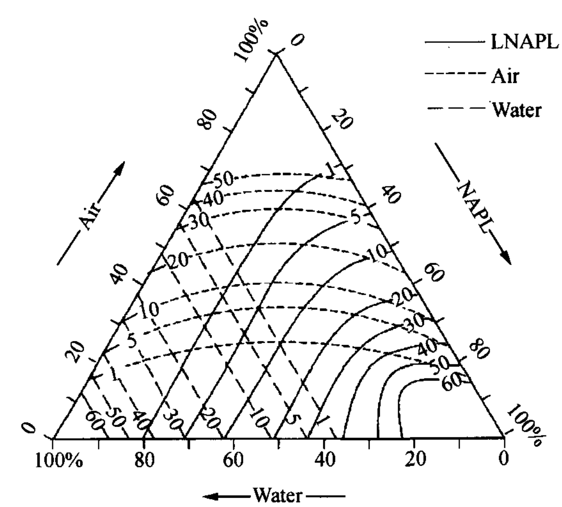

Fig. 4. Relative permeability for the three-phase flow in a ternary diagram.

If we assume that the wetting and non-wetting phases become spatially segregated to the extent that their relative permeability functions become dependent only upon their respective saturations, the permeability for each fluid phase can be derived according to Van Genuchten *S-P* model[18] and Mualem *k-S* model[26] as the following:

$$k_{rW}(S_W) = (S_{eW})^{\xi}\{1 - [1 - (S_{eW})^{1/m}]^m\}^2, \quad (4)$$

$$k_{rG}(S_G) = (S_{eG})^{\psi}\{1 - [1 - (S_{eG})]^{1/m}\}^{2m}, \quad (5)$$

$$k_{rN}(S_W, S_G) = (S_{eN})^{\zeta}\{[1 - (1 - S_{eTn})^{1/m}]^m - [1 - (S_{eTw})^{1/m}]^m\}^2, \quad (6)$$

where m is the *S-P* model parameter for the water-air system, and ζ, ψ and ξ are fitting parameters. The subscript e indicates the effective saturation.

However, the functional relationships of the relative permeability (k_r) of fluids (air, NAPLs, and water), saturation (S), and pressure (P) are non-linear and their direct experimental determination is very difficult. As indicated above, the relative permeability of each fluid in three-fluid flow system is commonly derived from the two-fluid problem based on simplified assumptions, therefore it is needed to obtain physical modeling results to complement and verify the numerical simulation of the multiphase flow.

A finite element method (FEM) numerical model - NAPL Simulator - is adopted to simulate the transport and fate of NAPLs in soils and groundwater[23]. The numerical solution is based on a Hermite collocation finite element discretization, and a sequential solution procedure is used to solve the coupled balance equations. This software can model the multiphase flow in porous medium, including capillary pressure, velocity and saturation of each fluid phase. For verification of the numerical data, centrifuge tests have been conducted to investigate the transport behavior of LNAPLs in subsurface system.

2 Numerical simulation of LNAPL transport

Using the FEM software, the air-LNAPL-water multi-phase flow in subsurface system is modeled, and the transport behavior of LNAPL is investigated in terms of migration pattern, tempo-spatial distribution in soils and groundwater, and contamination extent, under different boundary conditions.

The calculation model of LNAPL transport in the subsurface system is shown in Fig. 5. Fine sand mass was used as an unsaturated zone, and the aquifer was modeled by coarse sands. Their physical properties are listed in Table 2. They were also used in the centrifugal tests in this study. Ethyl-benzene was adopted as LNAPL, and its physical properties are listed in Table 3. Initially the soil was saturated by water. At the beginning of the numerical modeling, the soil was drained until reaching a stable moisture profile. Then, LNAPL was injected into the unsaturated soil mass, which then migrated into the unsaturated zone. The injection rate was $0.0375\,cm^3/s$, and the injection lasted for about 4 months. The total injection of LNAPL was $0.38\,m^3$. LNAPL continued to migrate in the subsurface system when the LNAPL supply stopped after LNAPL was depleted. Two types of boundary conditions were adopted: the groundwater table was stationary in one case, and groundwater flowing from right to left at the velocity of 2.0×10^{-3} m/s was the other.

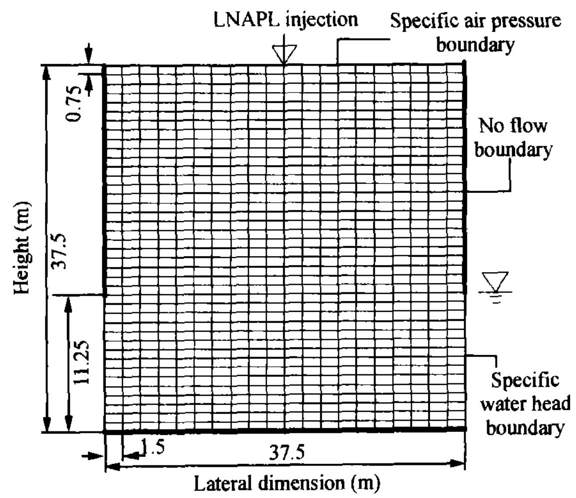

Fig. 5. Calculation model: LNAPL transport in the subsurface system.

Table 2. Physical properties of soil

Soil type	Porosity	Dry density	Intrinsic permeability
Fine sand	0.42	1.67 (g/cm^3)	1.46×10^{-11}(m^2)

Table 3. Physical properties of air, LNAPL and water

Fluid phase	Density (g/cm^3)	Dynamic viscosity (Pa·S)	Surface tension (g/cm)
Air	0.001196	0.0001785	/
LNAPL (Ethyl-benzene)	0.8670	0.0056	0.0449 (LNAPL-Water)
Water	1.0	0.01009	0.0742

2.1 LNAPLs transport in subsurface system with stationary groundwater

Fig. 6 shows distribution of LNAPL after its migration in the subsurface system for 1, 2, 3 and 5 years. The groundwater is stationary, and the groundwater table is located on the top of aquifer. Fig. 7 shows the LNAPL distribution in groundwater at different time. Numerical results show that LNAPL moves downwards first and is retained to form a high concentration zone on top of the capillary fringe. The long-term migration behavior is also predicated by numerical modeling, demonstrating that LNAPL accumulates and spreads laterally along the capillary fringe.

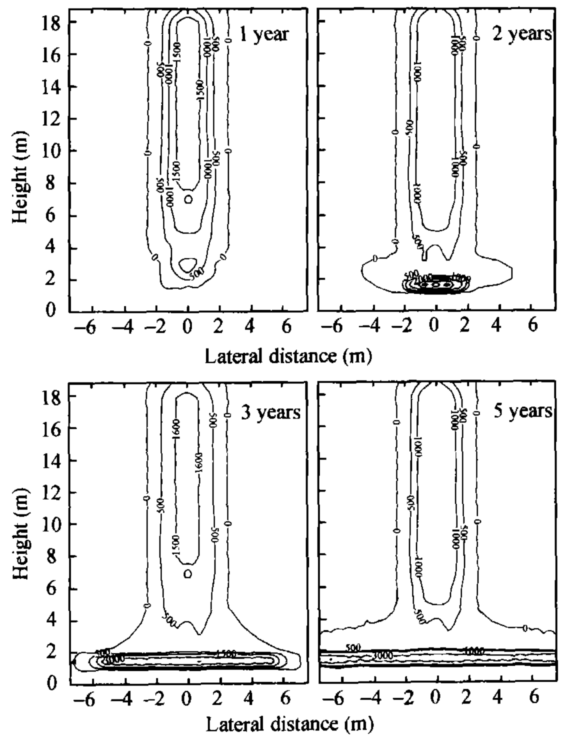

Fig. 6. Numerical results of tempo-spatial concentration of LNAPL in unsaturated soil (Unit: ppm).

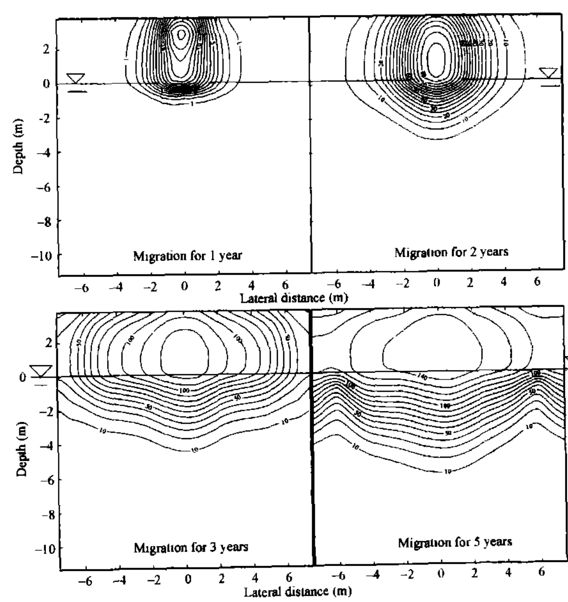

Fig. 7. Numerical results of tempo-spatial concentration of LNAPL in groundwater (Unit: ppm).

2.2 LNAPLs transport in subsurface system with groundwater flow

Fig. 8 and Fig. 9 show the calculated results for spatial distribution of LNAPL after 1, 2, 3 and 5 years' migration in unsaturated soils and groundwater system. Groundwater flows from right to left at the velocity of 2.0×10^{-3} m/s.

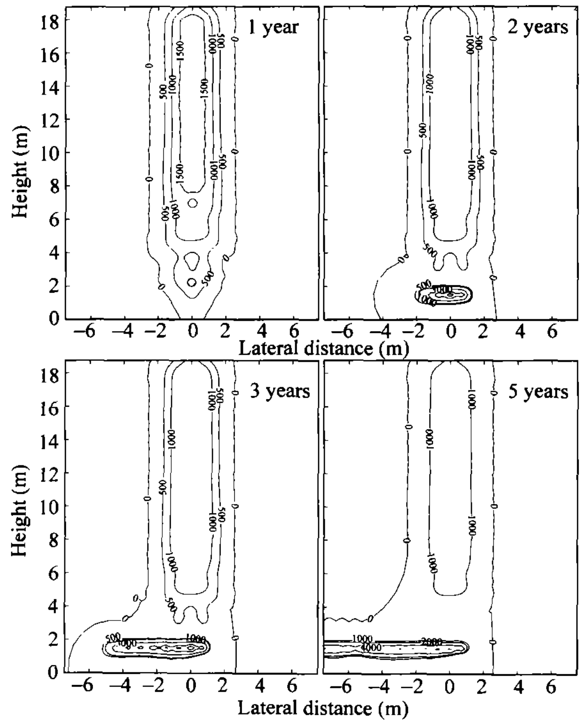

Fig. 8. Numerical results of tempo-spatial concentration of LNAPL in unsaturated soils (Groundwater flow) (Unit: ppm).

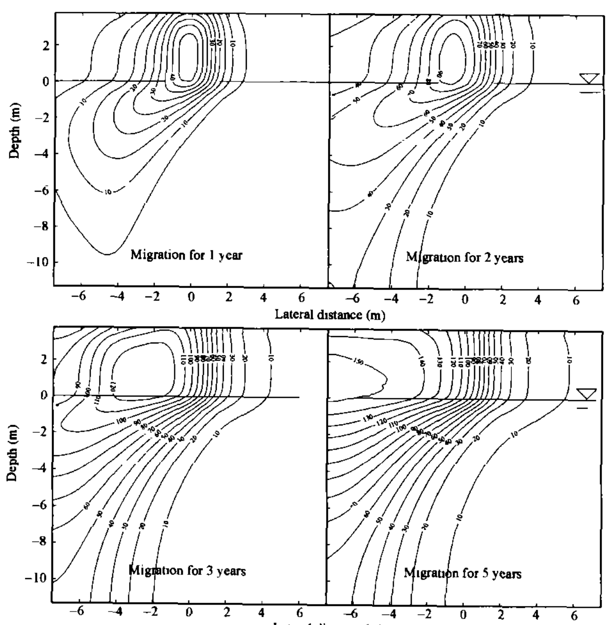

Fig. 9. Numerical results of tempo-spatial concentration of LNAPL in groundwater (Groundwater flow) (Unit: ppm).

It is shown that groundwater flow has little influence on transport behavior before LNAPL reaches groundwater table. However, after LNAPL reaches the groundwater table and starts migration in groundwater, the transport pattern in groundwater system is remarkably affected by groundwater flow, which also has impact on LNAPL distribution in unsaturated soils due to movement of the free phase with groundwater flow.

2.3 Discussion

Although numerical method has many advantages in modeling the long-term process and simulating various boundary/initial conditions, it requires verification of laboratory testing or field investigation. Conventional laboratory column tests, though relatively uncomplicated to perform, are often found to be inadequate for simulating site conditions and the long-term transport of LNAPLs in the unsaturated zone and groundwater. Centrifugal modeling seems to be a powerful physical modeling technique for geo-environmental engineering problems. In this study, the centrifugal tests were performed to verify the calculation results of numerical methods.

3 Centrifugal modeling of LNAPL transport

A geotechnical centrifuge can be used to perform tests on models that represent full-scale prototypes under normal field conditions. A $1/N$ scale model tested at a centrifugal acceleration N times that of the earth's gravity experiences the stress conditions identical to those of the prototype. Fluid flow occurs N times faster in a centrifuge model. In geo-environmental engineering, it is important to speculate on the fate of pollutant and on their long-term environmental impact. The use of a centrifuge can be a powerful physical modeling technique to study the long-term pollutant transport in soils.

3.1 Centrifugal testing model

The centrifugal tests were conducted to simulate LNAPL transport in unsaturated fine sands at a 75 g level in the Geotechnical Centrifuge Laboratory at Tsinghua University, which has an effective radius of 2 m and a payload capacity of 50 g-ton with a maximum acceleration of 250 g.

Ethyl-benzene was adopted as LNAPL in the centrifugal test. According to the numerical model, fine sands (British Standard Fraction E) were used in preparation of the unsaturated soil samples, which were uniform quartz sands with a mean diameter D_{50} of 0.12 mm. The intrinsic permeability was 1.46×10^{-11} m^2. Coarse sands with a mean diameter D_{50} of 0.40 mm were used as the aquifer material.

A strongbox was made of steel with a 50 mm thick plexiglas front. The groundwater could be maintained stationary or flowing at the velocity of 2.0×10^{-3} m/s. A two-chamber container was designed to release LNAPLs automatically when the centrifuge acceleration reached the desired g level as an underground storage tank for LNAPLs[6]. The groundwater sampling system with twelve syringes was installed in the strongbox, which could collect water samples during centrifuge flight by use of a driving piston connected with syringes. After LNAPL migrated in soils for one year (prototype time), the centrifuge stopped and soil samples were collected for detection of contaminants by gas-chromatography. The centrifugal tests were designed to match the numerical model as well as initial and boundary conditions. The used strongbox is shown in Fig. 10.

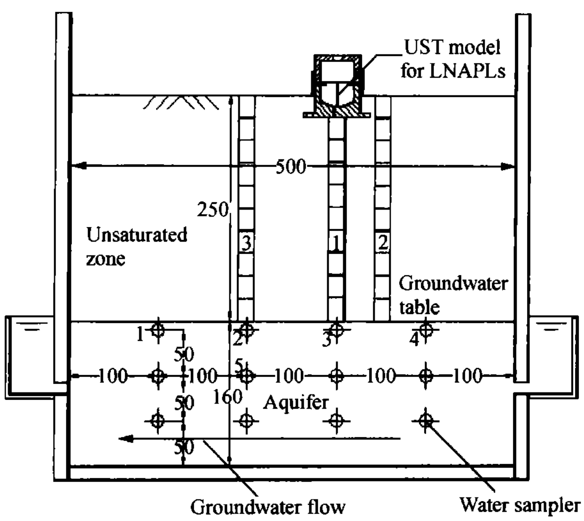

Fig. 10. Schematic of strongbox designed for centrifugal tests (Unit: mm).

3.2 Centrifugal test results for stationary groundwater table

The spatial distribution of LNAPL after one year migration with stationary groundwater is shown in Fig. 11. LNAPL concentration in water phase is shown in Fig. 12. LNAPL moves downwards and spreads laterally 4 m away from the leaking point. Then LNAPL is retained by the capillary fringe and forms a high concentration zone on the top of the capillary fringe. Some dissolved LNAPL enters into the groundwater.

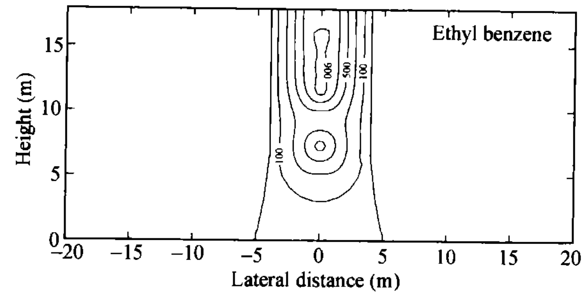

Fig. 11. Centrifugal test results: spatial distribution of LNAPL concentration in unsaturated soil after 1-year migration (Stationary groundwater table) (Unit: ppm).

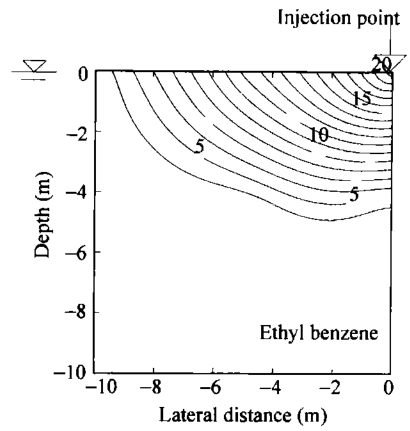

Fig. 12. Centrifugal test results: spatial distribution of LNAPL concentration in water phase after 1 year migration (Stationary groundwater table) (Unit: ppm).

It can be predicted that LNAPL will continue to transport along the capillary fringe and more dissolved components will migrate in groundwater system.

3.3 Centrifugal test results for groundwater flowing

Fig. 13 and Fig. 14 show the spatial distribution of LNAPL in the unsaturated zone and water phase after one year migration with groundwater flowing. Apparently, groundwater flow expedites the transport of LNAPL in subsurface system. Although the LNAPL spatial distribution in upper part of the unsaturated zone is little affected by the groundwater flow, the contamination pattern near the capillary fringe differs very much from that under the stationary groundwater condition. In groundwater system, the hydrodynamic dispersion due to water flow greatly accelerates migration of dissolved LNAPL, and the contaminated area is much larger. Similar findings are also obtained by numerical modeling.

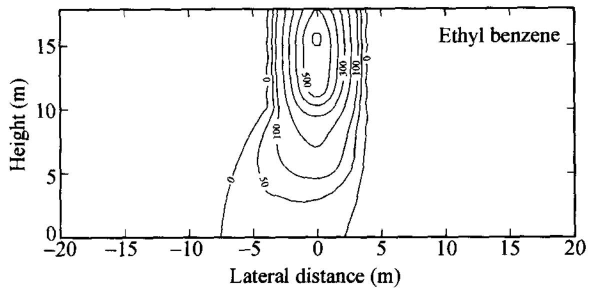

Fig. 13. Centrifugal test results: spatial distribution of LNAPL concentration in unsaturated soil after 1-year migration (Groundwater flow) (Unit: ppm).

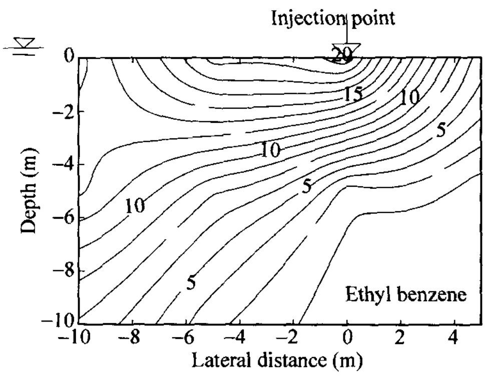

Fig. 14. Centrifugal test results: spatial distribution of LNAPL concentration in water phase after 1 year migration (Groundwater flow) (Unit: ppm).

3.4 Discussion

The centrifugal modeling and numerical simulation give the similar transport behavior in subsurface system: LNAPL moves downwards, forms a high concentration zone on the top of the capillary fringe, and then spreads laterally. Groundwater flow will expedite LNAPL migration, especially in groundwater system. Because the volatilization feature of LNAPL is not adequately reflected in the numerical solution, contamination extent in the unsaturated zone is less than that obtained by centrifugal tests.

4 Summary and conclusion

This paper presents results of numerical simulation and centrifugal tests on LNAPLs migration in subsurface system. The following conclusions can be drawn from the current work:

(i) Numerical simulation has been successfully used to predict the transport process and distribution of LNAPLs in soils. Centrifugal test provides reliable results and can be used for verification of numerical data. The combination of numerical simulation and centrifugal modeling can be a useful means to study the subsurface transport of LNAPLs.

(ii) Results from numerical simulation and centrifugal test show that LNAPLs move downwards in the soil-air-water system due to the gravity force. When reaching the capillary fringe zone, LNAPLs are retained and form a high concentration zone, and then spread laterally.

(iii) Groundwater flow has an apparent effect on LNAPL migration and contamination extent, since free phase LNAPL will float above capillary fringe and move with groundwater, and dissolved LNAPL will transport much faster due to hydrodynamic dispersion. The intrinsic permeability of soil plays a significant role in migration behavior of LNAPLs, while the residual saturation of LNAPL is correlated with contamination extent.

Acknowledgements The authors thank Mr. Yin Kunting and Mr. Hao Rongfu for their tremendous assistance throughout the centrifugal tests at Tsinghua University. The valuable suggestion on numerical simulation from Dr. Guarnaccia at Columbia University is greatly appreciated.

References

1 Van der Heijde P. K. M., El-Kadi A. I. and Williams S. A. Groundwater modeling: an overview and status report. USEPA, Ada, OK, 1988.
2 Wipfler E. L., Ness M., Breedveld G. D. et al. Infiltration and redistribution of LNAPL into unsaturated layered porous media. Journal of Contaminant Hydrology, 2004, 71(1—4): 47—66.
3 Illangasekare T. H., Znidarcic M., Al-Sheridda et al. Multiphase flow in porous media. In: Centrifuge 91. Rotterdam: Balkema, 1991, 517—523.
4 Knight M. A. and Mitchell R. J. Modeling of Light non-aqueous phase liquid (LNAPL) releases into unsaturated sand. Canadian Geotechnical Journal, 1996, 33(6): 913—925.
5 Esposito G., Allersma H. G. B. and Selvadurai A. P. S. Centrifuge modeling of LNAPL transport in partially saturated sand. Journal of Geotechnical and Geoenvironmental Engineering, ASCE, 1999, 125(12): 1066—1071.
6 Hu L. M., Shu S. Z., Lo I. M. C. et al. Centrifuge modeling of LNAPLs in porous media. In: Inter. Conf. Physical Modeling in Geotechnics—ICPMG ' 02. Rotterdam: Balkema, 2002, 367—372.
7 Culligan P. J., Banno K., Barry D. A. et al. Preferential flow of a nonaqueous phase liquid in dry sand. Journal of Geotechnical and Geo-environmental Engineering, ASCE, 2002, 128(4): 327—337.
8 Soga K., Kawabata J., Kechavarzi C. et al. Centrifuge modeling of non-aqueous phase liquid movement and entrapment in unsaturated layered soils. Journal of Geotechnical and Geo-environmental Engineering, ASCE, 2003, 129(2): 173—182.
9 Lo I. M. C., Hu L. M. and Meegoda N. J. Centrifuge modeling of LNAPL transport in unsaturated soils. Journal of Geotechnical and Geoenvironmental Engineering, ASCE, 2004, 130(5): 535—539.

10 Lo I. M. C., Hu L. M. and Meegoda J. N. Feasibility study of using centrifuge for investigating LNAPL migration in unsaturated soils. Soil & Sediment Contamination, 2005, 14(1): 85—103.

11 Wong R. C. K. Effects of clay content and temperature on crude oil (nonvolatile components) transport in unsaturated soils: Centrifuge study. Journal of Environmental Engineering, ASCE, 2005, 131(10): 1473—1478.

12 Arulanandan K., Thompson P. Y., Kutter B. L. et al. Centrifuge modeling of transport processes for pollutants in soils. Journal of Geotechnical Engineering, ASCE, 1988, 114(2): 185—205.

13 Culligan-Hensley P. J. and Savvidou C. Environmental geotechnics and transport processes. In: Geotechnical Centrifuge Technology. London: Blackie Academic & Professional, 1995, 196—263.

14 Pinder G. F. and Abriola S. C. On the simulation of non-aqueous phase organic compounds in the subsurface. Water Resources Res., 1986, 22: 109—119.

15 Richards L. A. Capillary conduction of liquids through porous mediums. Physics, 1931, 1: 318—333.

16 Brooks R. H. and Corey A. T. Hydraulic properties of porous media. Colorado State University, Hydrol. Pap., 1967, 3: 27—32.

17 Stone H. L. Estimation of three-phase relative permeability and residual oil data. J. Canadian Pet. Tech., 1973, 12(4): 53—61.

18 Van Genuchten M. T. A closed-form equation for predicting the hydraulic conductivity of unsaturated soils. Soil Sci. Soc. Amer. Journal, 1980, 44: 892—898.

19 Fredlund D. G. and Xing A. Q. Equations for soil-water characteristic curve. Can. Geo. Journal, 1994, 31(4): 521—532.

20 Parker J. C. and Lenhard R. J. A model for hysteretic constitutive relations governing multiphase flow. Water Resources Res., 1987, 23: 2187—2196.

21 Lenhard R. J. and Parker J. C. Experimental validation of the theory of extending two-phase saturation-pressure relations to three-fluid phase systems for monotonic drainage paths. Water Resour. Res., 1988, 24(3): 373—380.

22 Lenhard R. J., Oostrom M. and Dane J. H. A constitutive model for air—NAPL—water flow in the vadose zone accounting for immobile, non-occluded (residual) NAPL in strongly water-wet porous media. Journal of Contaminant Hydrology, 2004, 71: 261—282.

23 Guarnaccia J., Pinder G. and Fishman M. NAPL: Simulator Documentation, USEPA, EPA/600/R-97/102, 1997.

24 Gardner W. R. Some steady-state solutions of the unsaturated moisture low equation with application to evaporation from a water table. Soil Science, 1958, 85: 228—232.

25 Kunze R. J., Uehara G. and Graham K. Factors important in the calculation of hydraulic conductivity. Soil Science Society of America, 1968, 32: 760—765.

26 Mualem Y. A new model for predicting the hydraulic conductivity of unsaturated porous media. Water Resources Res., 1976, 12: 513—522.

27 Fredlund D. G., Xing A. Q. and Huang S. Y. Predicting the permeability function for unsaturated soils using the soil-water characteristic curve. Can. Geo. J., 1994, 31: 533—546.

28 Reddi L. N. and Inyang H. I. Geo-environmental Engineering: Principles and Applications. London: Marcel Dekker, Inc., 2001.

29 McWhortor D. B. and Sunada D. K. Exact integral solutions for two-phase flow. Water Resources Res., 1990, 26(3): 399—413.